Chemistry Europe
European Chemical Societies Publishing

WILEY VCH

Excellence in Chemistry Research

Announcing our new flagship journal

- Gold Open Access
- Publishing charges waived
- Preprints welcome
- Edited by active scientists

Meet the Editors of *ChemistryEurope*

Luisa De Cola
Università degli Studi di Milano Statale, Italy

Ive Hermans
University of Wisconsin-Madison, USA

Ken Tanaka
Tokyo Institute of Technology, Japan

ChemPlusChem

Research Article
doi.org/10.1002/cplu.202200313

Chemistry Europe
European Chemical Societies Publishing

www.chempluschem.org

Self Cycloaddition of *o*-Naphthoquinone Nitrosomethide to (±) *Spiro*{naphthalene(naphthopyranofurazan)}-one Oxide: An Insight into its Formation

Demeter Tzeli,*[a, b] Ioannis E. Gerontitis,[c] Ioannis D. Petsalakis,[b] Petros G. Tsoungas,*[d] and George Varvounis[c]

2-Hydroxy-1-naphthaldehyde oxime was oxidized by AgO (or Ag_2O), in presence of N-methyl morpholine N-oxide (NMMO), to the title *spiro* adduct-dimer (±)-*Spiro*{naphthalene-1(2*H*),4′-(naphtho[2′,1′:2,3]pyrano[4,5-*c*]furazan)}-2-one-11′-oxide by a Diels-Alder(D–A) type self-cycloaddition, through the agency of an *o*-naphthoquinone nitrosomethide (*o*-NQM). Moreover, 2-hydroxy-8-methoxy-1-naphthaldehyde oxime was prepared and subjected to the same oxidation conditions. Its sterically guided result, 9-methoxynaphtho[1,2-*d*]isoxazole, was isolated, instead of the expected spiro adduct. The *peri* intramolecular H bonding in the oxime is considered to have a key contribution to the outcome. Geometry and energy features of the oxidant- and stereo-guided selectivity of both oxidation outcomes have been explored by DFT, perturbation theory and coupled cluster calculations. The reaction free energy of the D–A *inter*molecular cycloaddition is calculated at −82.0 kcal/mol, indicating its predominance over the *intra*molecular cyclization of *ca.* −37.6 kcal/mol. The cycloaddition is facilitated by NMMO through dipolar interactions and hydrogen bonding with both metal complexes and *o*-NQM. The 8(*peri*)-OMe substitution of the reactant oxime sterically impedes formation of the spiro adduct, instead it undergoes a more facile cyclodehydration to the isoxazole structure by *ca.* 4.9 kcal/mol.

Introduction

Suitably functionalized privileged structures,[1] used as pharmacophoric scaffolds,[2] are major players in the quest for effective drug leads. *ortho*-Quinone methides (*o*-QMs) are well-known[3] transient reactive intermediates of a dearomatised structure, featuring an α,β-unsaturated enone and an exocyclic alkene (Scheme 1, **A**).

Their generation from suitable precursors by numerous methods and their structure and chemistry have been covered in many reviews over the years.[3–5] Commonly used methods for their *in situ* generation are thermolysis, photolysis, tautomerization, acid- or base-triggered transformations, 6π-electrocyclisation, oxidation by heavy or transition metal reagents or by hypohalites.[3] Their high reactivity rests upon their tendency to rearomatise ("revert to type"), mainly through Michael additions onto the enone segment. Diels-Alder (D–A) type cycloadditions, on the other hand, build up spiro adducts (spirocycles),[4,5] core units in natural products, many of which are important in therapeutics, including antibiotics and anti-tumour drugs.[3] The fate of *o*-QMs in a reaction medium often depends on their concentration. Thus, at a relatively high concentration, in the absence of an external stimulus (a nucleophile or an electron-rich diene/dienophile), *o*-QMs are known[5] to undergo dimerization or trimerization (Scheme 1, *spiro* adducts dimer **B** and trimer **C**).

The nitroso variant of *o*-QMs, *o*-quinone nitrosomethide (*o*-NQMs), generated and described in our early reports,[6,7] encompasses a β-*nitroso*alkene and the *o*-quinone methide entity (Scheme 1, **D**). In those reports, *o*-NQMs, by analogy to their parent structure, have been proposed as transiently generated during the oxidation of *o*-hydroxyaryl acyloximes.[6,7] Features of their geometry, reflected on their reactivity profile, have been detailed in our recent reports.[8,9]

The nitroso (NO) group is a well-documented[10] component of cycloadditions. The nitrosoalkene arm of *o*-NQM, on the other hand, is an effective heterodiene in D–A cycloadditions,

[a] *Prof. D. Tzeli*
Laboratory of Physical Chemistry
Department of Chemistry
National and Kapodistrian University of Athens
Panepistimiopolis Zografou Athens
157 84, Athens (Greece)
E-mail: tzeli@chem.uoa.gr
[b] *Prof. D. Tzeli, Dr. I. D. Petsalakis*
Theoretical and Physical Chemistry Institute
National Hellenic Research Foundation
48 Vassileos Constantinou Ave.
Athens 116 35 (Greece)
[c] *I. E. Gerontitis, Prof. G. Varvounis*
Section of Organic Chemistry and Biochemistry
Department of Chemistry
University of Ioannina
451 10 Ioannina (Greece)
[d] *Dr. P. G. Tsoungas*
Department of Biochemistry
Hellenic Pasteur Institute
127 Vas. Sofias Ave.
115 21 Athens (Greece)
E-mail: pgt@otenet.gr

Supporting information for this article is available on the WWW under https://doi.org/10.1002/cplu.202200313

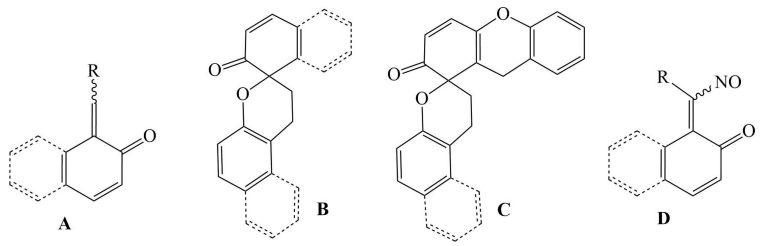

Scheme 1. *o*-QM **A**, its spiro adducts dimer **B** and trimer **C** and *o*-NQM **D** (in its E/Z conformations).

in which the NO group, in its E/Z conformations,[8,9] is an active participant.[10,11] Useful structures can be and have been prepared from *o*-NQMs, such as fused 1,2-oxazoles (isoxazoles) **6**[6–8] and 1,2-oxazines **4**[7–9] (Scheme 3). The isoxazole ring, fused to other rings, 3-substituted or 3,4-disubstituted with pharmacophores, is an established privileged structure and an area of active research with diverse applications. For instance, isoxazole-based marketed drugs, such as penicillin antibiotics (cloxacillin, dicloxacillin, flucloxacillin),[12] antipsychotics (risperidone, paliperidone),[13] COX2 inhibitors (e.g. parecoxib),[14] to name a few, are known. The profile of the long known,[15] structure **4**, on the other hand, has only recently started to be unveiled by our reports.[16]

The pyran ring, attached to arenes, either in a fused[17–19] or in a *spiro*[20] arrangement, is a known privileged structure.[21] It is a core unit in many natural products (e.g., eleutherins, kalafungins or nanaomycins) or natural product-like small molecules of biological and medicinal significance.[22] *Spiro* pyrans are used as optical probes in diagnostic imaging technology due to their chemilumin(fluor)escence properties[23] (Scheme 2). Their naphthalene analogues are also fundamental components in photochromic materials.[24,25]

The broad range of applications of arene-fused pyrans[26] and *spiro* pyrans[27] in materials technology and pharmaceutical industry[24,25] portrays their importance and the demand for efficient syntheses of new useful derivatives.

Currently available diagnostic imaging techniques are *limited* by *sensitivity* and *specificity*.[28] Reference standards in use are tedious and expensive (use of *in vitro* microsome series is often undesirable as it requires material from animal or human origin). The techniques are based on optical sensors probing biological events and their degradation pathways (metabolites) and transformed into a detectable signal. Commonly used techniques in oxidative (and/or nitrosative) stress (RONS) pathologies, detect extra (intra) cellular reactive oxygen species (ROS) but *not* reactive nitrogen species (RNS).

Our objective, the 1st stage of which is described in the present report, is (a) a simple, efficient, and cost-effective route to the title *spiro* structure and features that secure its reaction course, (b) explore its reactivity profile (regioselective and diverse functionalization) and (c) based on its reactivity results, use the structure for reactions with RONS-triggered chemical events, identifiable by spectroscopic techniques. The title structure will eventually be introduced as a candidate probe, evaluating its potential for the detection/measurement of (RONS) in oxidative stress conditions.[29]

Results and Discussion

D-A self cycloaddition-formation of spiro adduct

Oxidants, such as the one-electron lead(IV) acetate (LTA) or the two-electron, I(III) reagents phenyliodine diacetate (PIDA) and phenyliodine bis(trifluoroacetate) (PIFA) or I(V) reagent Dess-Martin periodinane (DMP), operating by the ligand coupling mechanism,[30] are commonly used in ring cyclizations.[31,32] On the other hand, the use of transition metal (TM) oxides, like AgO (or Ag_2O), has certain advantages over non-TMs, such as multiple oxidation states, coordination potential and some *d* with *s* and *p* orbital hybridization.[33] Their oxidant profile, depends on the structure to be oxidized and the relative M–O (M: Ag, Pb) bond dissociation enthalpy (BDE) of the transiently generated organoelement complex.

Oxidative cyclisation of aldoxime **2** (R=H) to *o*-NQM intermediate **3**, followed by a D–A type self-cycloaddition

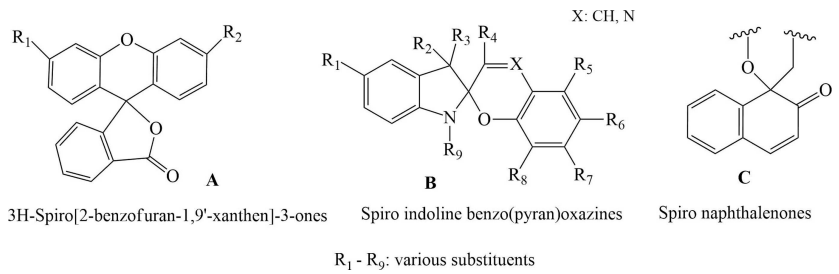

Scheme 2. Some spirocycles **a**-**c** used for the detection of small molecules.

(Scheme 3) furnishes the title *spiro* compound **5**. Of the oxidants previously used on **2**, $Pb(OAc)_4$ was found to be nonselective, giving all reaction products naphth[1,8-*de*]-1,2-oxazine **4**, *spiro* adduct **5** and naphth[1,2-*d*]isoxazole 2-oxide **6** (Scheme 3).[7] $PhI(OAc)_2$ and AgO (or Ag_2O), on the other hand, proved to be selective, furnishing **4** and **5** (Scheme 3), respectively.[6,7,34] Ketoximes **2**($R \neq H$), upon oxidative cyclisation with any of these oxidants, furnish the isolable C-3 substituted **6**.[6,7,35] In this redox economy-guided[36] sequence (Scheme 3), it is the geometry constraints in **3**,[8] mainly those of the exocyclic alkene, β- substituted or not and the oxidant profile that set the reaction course. **3** is common to these oxidations and eventually suffers an *o*- or *peri*-cyclisation[9] or the herein described cycloaddition (Scheme 3). Pertinent to its generation is the energy demanding, synthetically important oxidative dearomatization[37] of **2**, through an organoelement complex. The structure and reactivity profile of **3**[8,9] and its nitrosoalkene arm[6,7,38] have been detailed in our earlier reports.

Efficiently prepared **5** has been achieved by the use of AgO (or Ag_2O), in presence of *N*-methyl morpholine *N*-oxide (NMMO) (Scheme 4), by adapting an earlier method.[39] Without NMMO, the reaction led to a mixture of low yield unidentified products in aprotic solvents of varying polarity (e.g. THF, CH_2Cl_2 or MeCN). A commonly obtained yield of 40%, raised up to 46%, in a couple of attempts, was noted for **5** in CH_2Cl_2 and lower ones in the other solvents.

Earlier use of NMMO[40,41] targeted the extended lifetime of transient *o*-QM through a dipole-dipole stabilization. However, some *o*-QMs have been formed without the need of NMMO.[3,42,43]

The intramolecular H bond (IMHB)-driven pseudo ring conformation in oxime **2** (with a contribution from non-aromatic strained keto tautomer **2′**) triggers a redox relay by proton shuttling [Hydrogen AtomTransfer (HAT) or Proton Coupled Electron Transfer (PCET)][44–47] at the oxime and phenol OH sites (Scheme 5). This IMHB steers a metal coordination binding mode (Scheme 4, **7** or **7′**).[48] The dearomatizing tautomerization **2** to **2′** facilitates the development of a Ag complex[49] like **7** or its chelate **7′** (Scheme 4, routes (a) or (b), respectively). Indeed, **2**, acting as a monodentate or a bidentate

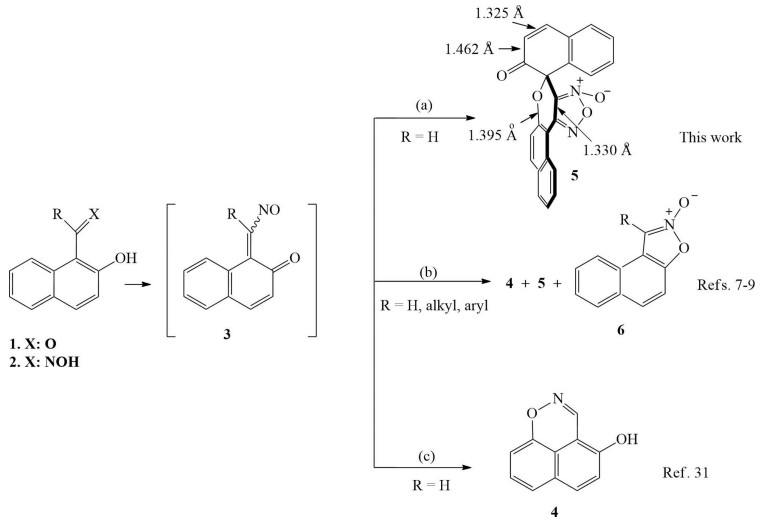

Scheme 3. (a) AgO (or Ag_2O), NMMO, NEt_3, CH_2Cl_2, r.t. (route a); (b) $Pb(OAc)_4$, CH_2Cl_2 or THF, 0 °C-r.t. (route b);(c) $PhI(OAc)_2$, *t*-BuOH, N_2, 0°-r.t. (route c).

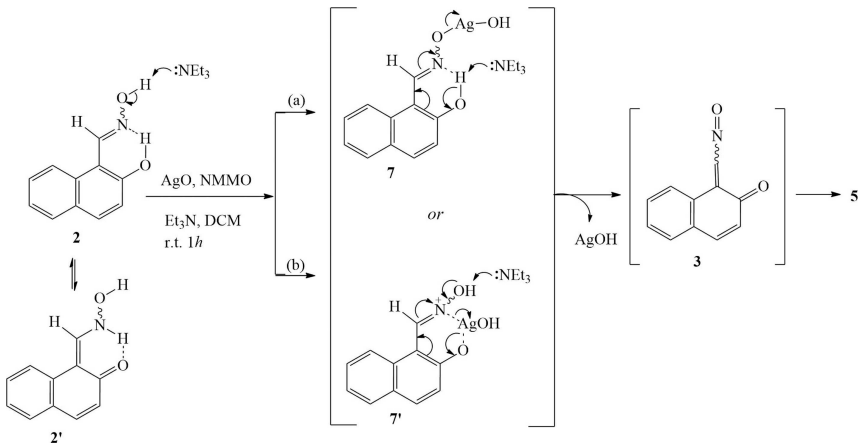

Scheme 4. A rationale for the selective AgO-NMMO oxidation of oxime **2**.

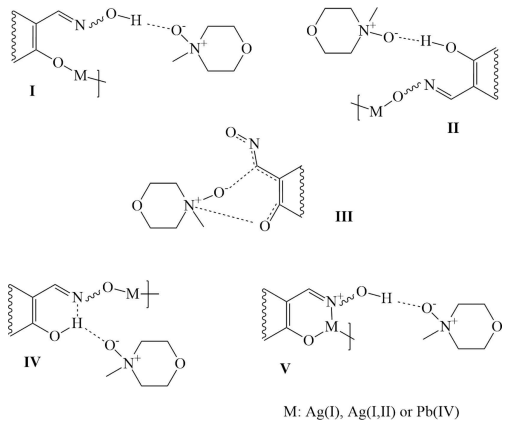

Scheme 5. Plausible interactions through Ag or Pb complexes.

ligand (Scheme 5, types **I**, **II** or **V**), coordinates with Ag, through a resonance-assisted IMHB chelate (Scheme 5, type **IV**)[50,51] or through a metal chelate (Scheme 5, type **V**). Their collapse, aided by NEt_3 (pKa = 10.75), generates **3** (Scheme 4). Interception of **3** by NMMO (Scheme 5, type **III**), probably extends its lifetime and renders self-D–A reaction to **5** as a viable outcome. Whether an *endo* or an *exo* approach, the stereochemistry of the D–A cycloaddition of **3** to **5** is of no significance. Furthermore, it is the *E*-conformer of **3** that effects the cycloaddition (the *Z*-conformer is in equilibrium with its isomeric *N*-oxide **6** R = H[9]).

DFT(B3LYP), MP2, MP4SDQ and CCSD calculations show that the **3**→**5** cycloaddition is an exoenergetic reaction in the presence of either Ag or Pb, see Tables 1 and 2. B3LYP data on the *intra*molecular **3**→**4** reaction and **3**→**5** *inter*molecular cycloaddition are in agreement with MP4SDQ and CCSD results. B3LYP and MP2, on the other hand, overestimate the reaction energy for the **3**→**6** *intra*molecular reaction compared with the CCSD data. Our previous studies on *intra*molecular cyclization of o-NQM **3** have shown that B3LYP, M06-2X and MP2 using the 6-311 + G(d,p) and aug-cc-pVTZ[9] sets predict similar results. It should be noted that the objective of the present investigation is the features governing the *inter*molecular cycloaddition, and this is satisfactorily predicted by the B3LYP/6-311 + G(d,p) methodology compared to the other ones, see Table 1.

The reaction free(Gibbs) energies are almost the same using both THF and CH_2Cl_2 solvents, see Table 2. It is found that the reaction free energy of the *intra*molecular **3**→**4** cyclization is −37.6 kcal/mol, while the *inter*molecular **3**→**5** reaction is a more exothermic one. Its reaction free energy is up to −82.0 kcal/mol depending on the reaction method, see Table 2. Thus, the *inter*molecular cyclization is apparently more favored, in agreement with the experimental findings.

The alternative *peri* cyclization to **4**, a result of free rotation of the Ag complex **7** (Scheme 4) is not an option as in the case of $Pb(OAc)_4$.[7,9] This is due to the M–O bonding (M: Ag or Pb) of the transient organometal complexes and their interaction with NMMO (Scheme 5 and Table 3). NMMO forms H bonds with Ag and Pb-complexes (Scheme 5, **I**, **II**, **IV** and **V**) and dipolar interactions with **3** and **3′** conformers (Scheme 5, **III**). It also facilitates their collapse and cycloaddition of **3** to the *spiro* structure **5**.

The O–Ag and O–Pb bond distances are found shorter by *ca.* 0.03 Å, when Ag or Pb are attached to the phenol O site (Scheme 5 and Table 3) than if attached to the oxime NO group. A BDE value of 5.7 kcal/mol (in **7** or **7′**) for Ag–O and BDE values of 26.2 kcal/mol (for **7**) and 34.4 kcal/mol (for **7′**) for the Pb–O complexes were found, respectively (Figure 1), regardless of the site of attachment. It is noted that positive BDE values means that the system is stable. It should be mentioned that Pb forms stronger bonds than Ag because it has half-filled d orbitals while Ag has all its d orbitals occupied.

NMMO appears to interact preferably with the metal complex of **7** at the phenol site (O–M…NMMO) (see Scheme 5). The BDE between NMMO and Pb and Ag complexes are *ca.* 28.3 kcal/mol and *ca.* 10.7 kcal/mol, respectively, indicating that the latter, i.e., Ag-complex…NMMO, is more prone to collapse. The Pb complexes with NMMO seem to be more stable because of multiple interactions, including H bonding, see Figure 1,

Table 1. Reaction energies ΔE for cyclization structures of **3** to **6**(*o-(1,5)-intra*molecular cyclization), **4** (*peri-(1,6)-intra*molecular cyclization), and **5**(*inter*molecular D–A type cycloaddition) in the gas phase at B3LYP, MP2, MP4SDQ and CCSD/6-311 + G(d,p).

	ΔE			
	B3LYP	**MP2**	**MP4SDQ**	**CCSD**
3→6	−14.0	−16.8	−4.3	−6.0
3→4	−39.4	−41.7	−36.6	−38.0
3→5[a]	−46.5	−61.0	−42.6	
3→5[b]	−71.9	−85.4	−75.9	

[a] In the presence of AgO(or Ag_2O) **3**→ **5**; **3** + **3** + Ag_2O→ **5** + AgOH + AgH. [b] In the presence of $Pb(OAc)_4$ **3**→ **5**; **3** + **3** + $Pb(OAc)_4$→ **5** + $Pb(OAc)_2$ + 2AcOH.

Table 2. Reaction enthalpies ΔH and free energies ΔG for cyclization structures of **3** to **6** (*o-(1,5)-intra*molecular cyclization), **3** to **4** (*peri-(1,6)-intra*molecular cyclization) and **3** to **5** (*inter*molecular D–A type cycloaddition) in the gas phase, THF (1) and CH_2Cl_2 (2) solvents.[a]

	ΔH	**ΔG**	**ΔH_1**	**ΔG_1**	**ΔH_2**	**ΔG_2**
3→6	−13.3	−11.3	−13.2	−11.2	−13.2	−11.2
3→4	−38.6	−36.9	−39.3	−37.6	−39.3	−37.6
3→5[b]	−48.0	−41.1	−54.2	−47.3	−54.3	−47.4
3→5[c]	−70.4	−78.0	−74.2	−81.0	−74.3	−82.0

[a] At the B3LYP/6-311G + (d,p) level of theory, in kcal/mol; ΔH and ΔG values are calculated at T = 298.15 K and P = 1 Atm. [b] In the presence of AgO(or Ag_2O) **3**→ **5**; **3** + **3** + Ag_2O→ **5** + AgOH + AgH. [c] In the presence of $Pb(OAc)_4$ **3**→ **5**; **3** + **3** + $Pb(OAc)_4$ → **5** + $Pb(OAc)_2$ + 2AcOH.

Table 3. M–O bond lengths [a] (Å) and M–O Bond dissociation energies BDE (kcal/mol)[a] of the complexes.

Metal complexes	M-O	BDE
7′-Ag	2.05 [2.03–2.5][b]	5.7
7-Ag	2.06	5.7
7′-Pb	2.08 [2.1–2.3][c]	34.4
7-Pb	2.05	26.2

[a] B3LYP/6-311 + G(d,p) level of theory. [b] Typical O…Ag bond distances, Ref. [52]. [c] Typical O…Pb(IV) bond distances, Ref. [53].

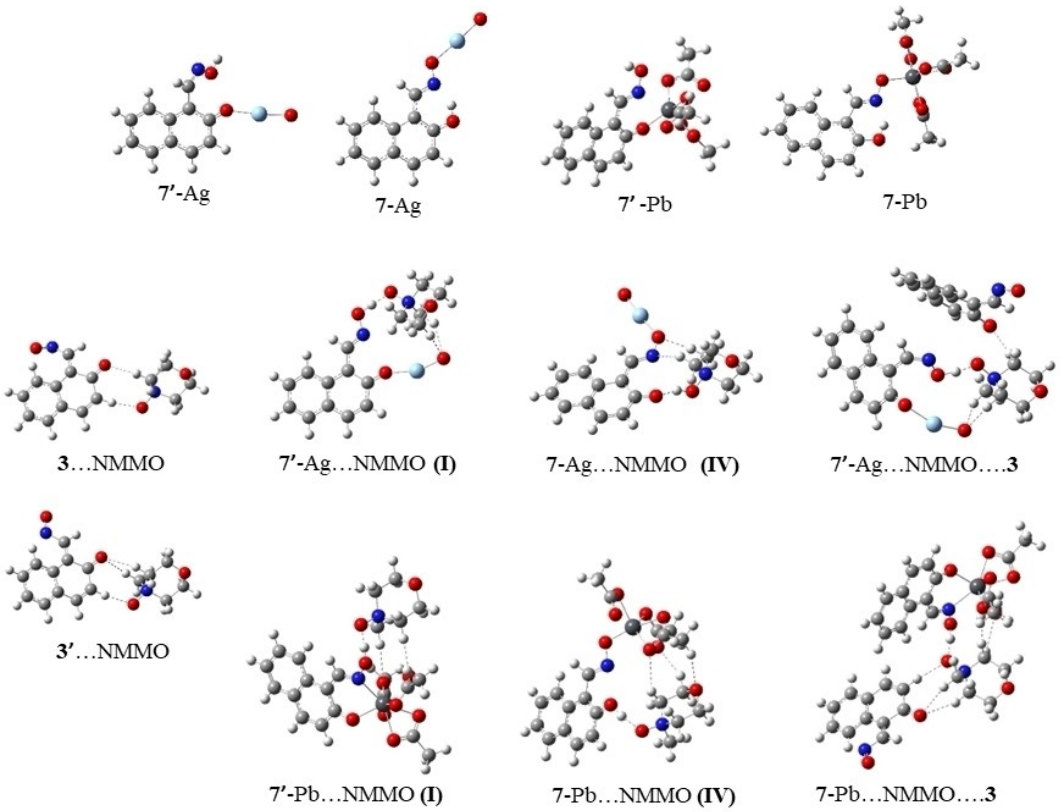

Figure 1. Calculated Ag and Pb complexes and their interaction with NMMO.

resulting to stronger bonding in Pb complexes compared to the Ag ones, see Table 4.

Compound **5** is a *spiro* 6-ring structure[7–9] around a C-sp^3 centre of a distorted planar tetrahedron bonded to a naphthalene-2-one (Scheme 6)[7–9] A 1,2,5-oxadiazole *N*-oxide (furoxan) ring is fused onto the pyran component of the naphtho[2,1-*b*]pyran. The alkene of 1.325 Å and the C–C of 1.462 Å bond lengths for the quinone domain (experimentally measured of 1.455 Å,[7–9] cf., with a single sp^2-sp^2 of *ca.*1.480 Å), indicate some weak conjugation between the two unsaturation sites. Worth noting is that the exocyclic alkene bond of **3** (1.363 Å and 1.369 Å for its two *E*-conformations)[8] compares well with the quinonoid alkene bond in **5**. A 1.395 Å length, notably shorter than a common C–O bond, is observed for the bond shared by naphthalene fused to the pyran ring. A double bond character of 1.330 Å is also clearly indicated for the furoxan-pyran fusion C–C bond, expectedly a result of an enhanced *N*-oxide dipole-induced π-electron delocalization within the heteroring.

Table 4. Bond dissociation energies BDE (kcal/mol)[a] of complexes and **3** with NMMO.

Interacting Complexes	BDE	
	Ag	Pb
7-M….NMMO → **7**-M + NMMO	5.31	10.7
7′-M….NMMO → **7′**-M + NMMO	10.40	28.3
7-M….NMMO…**3** → **7**-M + NMMO + **3**	15.34	25.3

[a] B3LYP/6-311 + G(d,p) level of theory.

Sterically-impeded formation of spiro compound

With the AgO (or Ag_2O)–NMMO oxidation of **2** to **5** established, attention was focused on repeating this reaction having the 8(*peri*)-position of **2** blocked by a OMe group, that is, using **8** (Scheme 6) as starting material. In this case, the reaction succumbs to steric gearing.

Accordingly, 1-naphthaldehyde **11** was *o*- and *peri*-methoxylated to **12** and subsequently selectively demethylated by aluminium chloride to 2-hydroxy-8-methoxy-1-naphthaldehyde **13** and 2-methoxy-8-hydroxy-1-naphthaldehyde **14** isomers, the latter as the major component[54] (Scheme 7, route (a)). Apparently, *peri* congestion flanks and exposes the 8-OMe group, facilitating its demethylation against its *o*-counterpart. A Gattermann formylation of 1,7-dihydroxynaphthalene **15** to 2,8-dihydroxy-1-naphthaldehyde **16**, the only known alternative route,[55] is clearly not recommended due to (a) the reagents used (HCN generation), (b) its low (*ca.* 20%) yield, (c) formation of regioisomers and (d) laborious isolation of **16** by steam distillation. Furthermore, methylation of **16** furnishes **12** instead of the desired **13** (Scheme 7, route (b)).

A chelation control-selective[56] *peri*-methylation of **16** was also attempted in CH_2Cl_2 to avert any solvent-driven H bonding

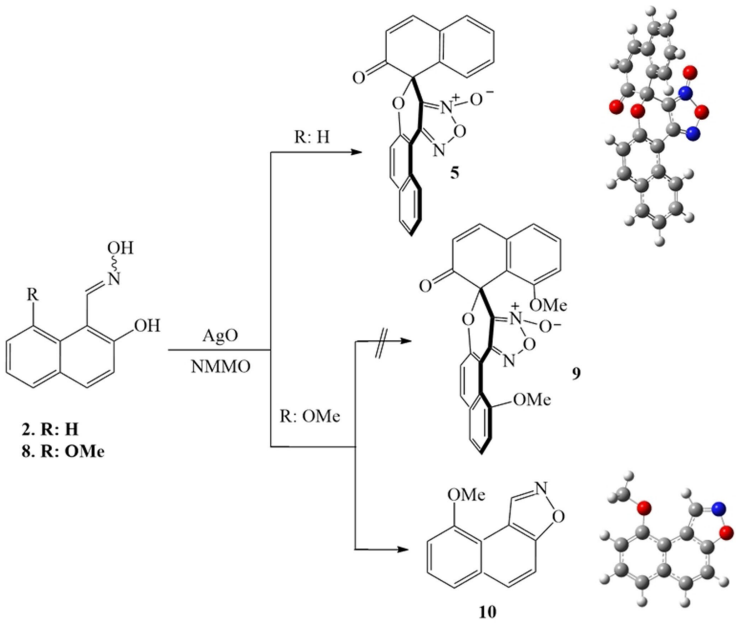

Scheme 6. A general representation of the effect of 8-(*peri*) substitution on the oxidation of **2** and **8**.

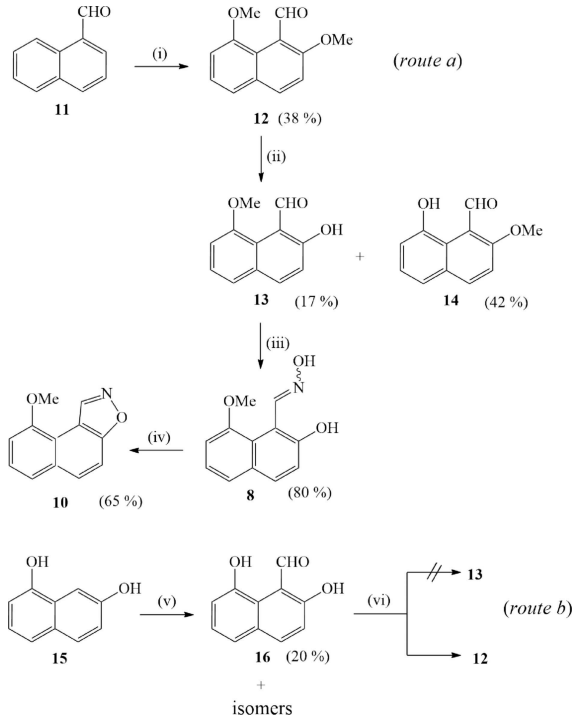

Scheme 7. (i) $Pb(OAc)_4$, MeOH, 3-$CF_3C_6H_4NH_2$, $K_2S_2O_8$, CH_2Cl_2, 60 °C, 24 h; **(ii)** (a)$AlCl_3$, CH_2Cl_2, 0 °C, (b) reflux, 2 h; **(iii)** (a)$NH_2OH.HCl$, MeOH, 0 °C, (b) Na_2CO_3 (sat.aq.) to pH 8, r.t.,1 h, (c)AcOH, 0 °C to pH 5; **(iv)** AgO, NMMO, NEt_3, CH_2Cl_2, r.t., 1 h (route (a)); **(v)** $Zn(CN)_2$, $HCl_{(g)}$, N_2, r.t.; **(vi)** MeI, K_2CO_3, DMF, r.t. or MeI, K_2CO_3,CH_2Cl_2, 30 min., r.t (route (b)).

interference and disruption of the *o*-IMHB. 2,8-Dimethoxylated **12** was the only major isolated product, suggesting that both *peri* 7-membered and *ortho* 6-membered IMHB in **16** are probably of comparable strength.

Aldehyde **13** was converted into oxime **8** (*E/Z* isomers), which, in turn, was subjected to oxidation with AgO, in the presence (or not) of NMMO and a catalytic amount of trimethyl -amine, to produce, after column chromatography, 9-methoxynaphtho[1,2-*d*] isoxazole **10**, in 65 % yield.**10** was identified from its NMR and HRMS spectra as well as its independent synthesis from the tosyl chloride and triethylamine cyclodehydration of oxime **8**.[57]

The inherent constraints of the reaction can be demonstrated by the stronger N…HO IMHB of **8** (1.680 Å) compared to the corresponding H bonding in **2** (Scheme 9). This is probably the result of the notable *peri* IMHB-triggered (2.006 Å) deformation in **8**, also indicative by their *peri* H–H distances of 2.430 Å and 2.359 Å, respectively. The resonance-assisted[58] N··HO IMHB and its *peri* MeO··HC=N counterpart, "lock" the reacting conformation of **8** into coplanarity (Scheme 8).

NMMO may facilitate, through **17**, formation and then collapse of Ag complexes like **18** or **20** and **21** to isoxazole **10** (Scheme 10). An *in plane* intramolecular nucleophilic substitution at the imine N atom as in **18**[59] or chelation as in **20** and further rearrangement to **21**,[60] trigger ultimate cyclodehydration to **10**.

A direct dehydration of **18** (path (b)), on the other hand, or isoxazole ring-opening in **10** (path (a)), by the well-known Kemp elimination,[61] to nitrile **19** was not detected. Indeed, an NMR C-1 H signal at $\delta = 9.6$ ppm, indicative of an IMHB, usually found at $\delta = 9.1$ ppm,[62] remained unaltered on deuteration.

The *peri* IMHB (2.520 Å, Scheme 8), engaging the C-1 H atom in **10**, inhibits ring rupture. A *peri* IMHB (2.198 Å)-driven deformation in **23** (*peri* H–H distance of 2.400 Å (Scheme 9) and a comparable deformation in **10** (*peri* IHB 2.520 Å, H–H 2.431 Å, Scheme 9), probably encourage the lower energy demanding cyclodehydration of oxime **8** to isoxazole **10**.

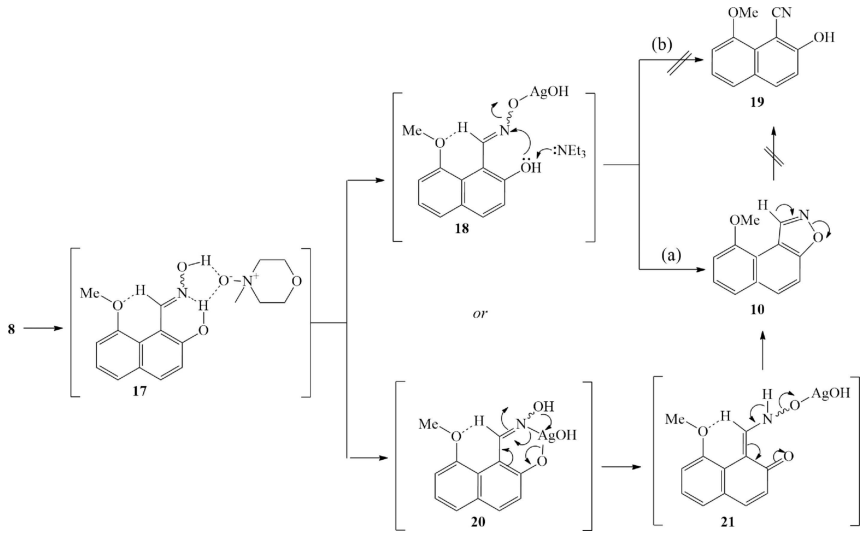

Scheme 8. A rationale for the oxidation of oxime **8**.

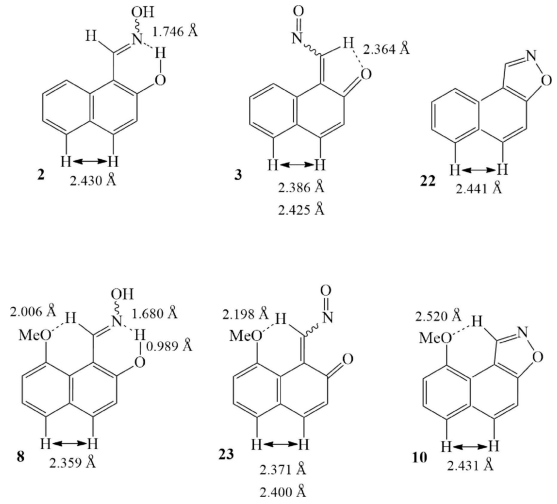

Scheme 9. Geometry data of reactants, intermediates and products in the oxidation of **2** and **8** (two isomers have been calculated for **3** and **23**) at B3LYP/6-311 + G(d,p).

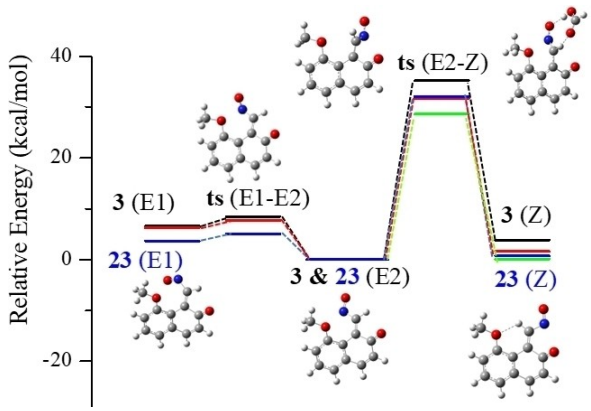

Figure 2. Relative energies of the reactants and intermediates for oxidation of **2** and **8** at B3LYP/6-311 + G(d,p) level of theory (black color for **3**, red color for **3** in the presence of MeOH, blue color for **23** and green color for **23** in the presence of MeOH).

The relative energies of the reactants, intermediates, transition states, and products of the oxidation of **2** and **8** are shown in Figure 2. **3** and **23** are depicted as their *Z* and *E* conformers with respect to the NO orientation (Figure 2). The presence of MeOH or EtOH[9] in solution can stabilize the transition states up to 4 kcal mol due to H bond interactions, see Figure 2. 8-methoxy substitution gives rise to more stable Z and E1 conformers of **23**, compared to those of **3** by *ca.*4.9 kcal/mol. Note that the energy gap for the E2→Z change is about 30 kcal/mol, lowered by about 4 kcal/mol, upon interaction of the transition state with MeOH.

1,2-benzisoxazole is known[63] to act as an N- or O-nucleophile in annulation reactions furnishing quinolones or isoquinolines. Thus, if treated with a protic solvent, an intermolecular H bonding[64] to any of the three available N or O sites of **10** (**A**, Scheme 9), might trigger its ring-opening to nitrile **19**. When **10** was stirred in MeOH or in MeOH-AcOH for 12 h remained intact. Worth noting, however, is that the *peri* IMHB of **10** is disrupted by K ion,[65] when treated with K_2CO_3 in DMSO, followed by a Kemp elimination[61] to **19** (**B**, Scheme 10).

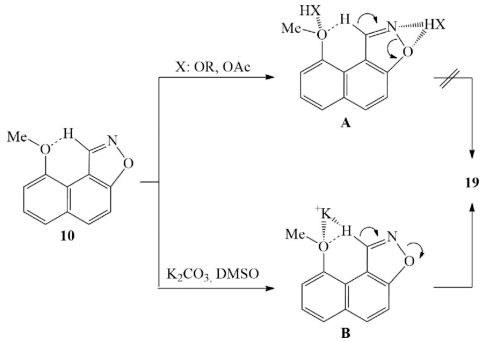

Scheme 10. A rationale for isoxazole opening to nitrile **19.**

Conclusion

2-Hydroxy-1-naphthaldehyde oxime can be selectively oxidized to a spiro adduct-dimer, encasing a pyranonaphthalenone structure, through the agency of an *o*-NQM by its D–A type self-cycloaddition. A *peri* OMe-substituted naphthaldoxime derivative, on the other hand, under the same oxidation conditions, fails to give the corresponding *spiro* adduct, owing to geometry constraints introduced by the *peri* substituent. Instead, the sterically geared reaction succumbs to a cyclodehydration leading to 9-methoxynaphtho[1,2-*d*]isoxazole. The *peri* intramolecular H bonding in the oxime does contribute to the outcome.

DFT, MP*n* and CCSD calculations show that *the inter*molecular cycloaddition is an exoenergetic reaction. The reaction Gibbs energy of this cycloaddition of *ca.* −82.0 kcal/mol is more favoured than the intramolecular reaction of *ca.* −37.6 kcal/mol. NMMO facilitates the cycloaddition through H bonding and dipolar interactions with both the metal complexes and *o*-NQM. The 8(*peri*)-OMe substituted reactant oxime undergoes a more facile cyclodehydration to the isoxazole structure by *ca.* 4.9 kcal/mol.

The α,β-unsaturated enone and the nitrosoalkene parts of the target *spiro* structure makes it susceptible to attack by nucleophiles (or electrophiles) and by analogy to reactive oxygen and nitrogen species (ROS, RNS).[66] It can, thus, serve as a candidate probe for the detection and measurement of these species in oxidative stress conditions. The susceptibility of *spiro* pyran to opening, on the other hand, makes the *spiro* structure a precursor to (a)symmetrically substituted 3,4-diarylfuroxans, known nitric oxide (NO) modulators in vascular endothelium pathology, related to the development of oxidative stress.

Experimental Details

Melting points were taken on a Büchi 510 apparatus and are uncorrected. ^{1}H and ^{13}C NMR spectra were measured in $CDCl_3$ or DMSO-d_6 on a 400 MHz Bruker spectrometer. ^{1}H chemical shifts are reported in ppm from an internal standard TMS, residual chloroform (7.26 ppm) or DMSO-d_6 (2.50 ppm). ^{13}C NMR chemical shifts are reported in ppm from an internal standard TMS, residual chloroform (77.16 ppm) or DMSO-d_6 (39.43 ppm). High resolution ESI mass spectra were measured on a ThermoFisher Scientific Orbitrap XL system. Low resolution ESI spectra were measured with an Agilent 1100 Series LC–MSD-Trap-SL spectrometer, using MeOH or MeCN as eluant. Analytical thin layer chromatography was performed with Merck 70–230 mesh silica gel TLC plates. Purification of reaction products was generally done by dry-column flash chromatography using Merck silica gel 60 and/or flash chromatography using Carlo Erba Reactifs-SDS silica gel 60. All reactions were carried out under a N_2 atmosphere. Solvents and reagents were used as received from the manufacturers (Acros, Alfa Aesar and Merck) except for THF, DCM, MeOH, EtOAc, hexane and toluene that were purified and dried according to recommended procedures. Organic solutions were concentrated by rotary evaporation at 23–40 °C under 15 Torr.

2,8-Dimethoxy-1-naphthaldehyde (12): A closed vessel with a magnetic stir bar was charged with 1-naphthaldehyde (6.4 mmol, 1 g, 1 equiv.), $Pd(OAc)_2$ (0.64 mmol, 143 mg, 0.1 equiv.), $K_2S_2O_8$ (12.8 mmol, 6.46 g, 2 equiv.) in air followed by DCM (10 mL), MeOH (128 mmol, 5 mL, 20 equiv.) and 3-(trifluoromethyl)aniline (2.56 mmol, 317 μL, 0.4 equiv.). The reaction mixture was then stirred at 60 °C for 24 h. Upon completion of the reaction (monitored by TLC), the reaction mixture was cooled to room temperature, filtered, quenched by a saturated solution of $NaHCO_3$ (25 mL) and extracted with DCM (3×25 mL). The combined organic extracts were washed with brine (25 mL), dried over anhydrous Na_2SO_4 and concentrated *in vacuo*. The crude residue was purified by flash column chromatography (EtOAc:hexane: 1:10) to give the title compound (415 mg, 30%) as a red oil; R_f = 0.32 (EtOAc:hexane: 1:4); spectroscopic data are in agreement with those reported in the literature;[54] ^{1}H NMR ($CDCl_3$, 400 MHz,): δ 10.74 (s, 1H), 7.86 (d, J = 9.1 Hz, 1H), 7.40 (d, J = 8.1 Hz, 1H), 7.31-7.29 (t, 1H), 6.86 (d, J = 7.7 Hz, 1H), 3.93 (s, 3H), 3.93 (s, 3H); ^{13}C NMR ($CDCl_3$, 100.6 MHz,): δ 195.07, 154.95, 154.69, 131.93, 130.15, 124.53, 122.00, 121.34, 121.12, 114.24, 57.12, 56.01.

2-Hydroxy-8-methoxy-1-naphthaldehyde (13): To a stirred solution of 2,8-dimethoxy-1-naphthaldehyde (0.33 mmol, 70 mg, 1 equiv.) in anhydrous DCM (10 mL) was added $AlCl_3$ (0.97 mmol, 130 mg, 3 equiv.) at 0 °C. The reaction mixture was then heated to reflux for 2 h after which TLC analysis had shown complete conversion of the starting material. The reaction mixture was then left to cool to room temperature, water (20 mL) was added, the organic layer was separated and the aqueous layer was extracted with DCM (3× 10 mL). The combined organic extracts were washed with brine (25 mL), dried over anhydrous Na_2SO_4 and concentrated *in vacuo*. The acquired crude residue was purified by flash column chromatography (EtOAc:hexane: 1:10) to give the title compound (20 mg, 15%) as a yellow solid; m.p. 68–70 °C; R_f = 0.54 (EtOAc: hexane: 1:4); ^{1}H NMR ($CDCl_3$, 400 MHz): δ 14.15 (s, 1H), 12.26 (s, 1H), 7.91 (dd, J = 8.1, 1.2 Hz, 1H), 7.34 (t, J = 7.9 Hz, 1H), 7.14 (d, J = 9.0 Hz, 1H), 7.08 (dd, J = 7.8, 1.2 Hz, 1H), 4.02 (s, 3H); ^{13}C NMR ($CDCl_3$, 100.6 MHz): δ 199.55, 166.07, 155.86, 138.69, 129.86, 124.16, 123.29, 122. 45, 120.06, 113.52, 109.43, 55.62; HRMS (ESI) m/z $[M+H]^+$ calcd. for $C_{12}H_{10}O_3$ 203.0708, found 203.0711.

(*E*)-2-hydroxy-8-methoxy-1-naphthaldehyde oxime (8): To a stirred solution of 2-hydroxy-8-methoxy-1-naphthaldehyde (20 mg, 0.099 mmol) in MeOH (5 mL), $NH_2OH.HCl$ (14 mg, 0.198 mmol) was added, and the resulting mixture was cooled to 0 °C, followed by the dropwise addition of a saturated Na_2CO_3 solution until pH = 8 and the reaction mixture was left stirring at room temperature for 1 h. TLC analysis had shown complete conversion of the starting material, so the solution was cooled to 0 °C, followed by the dropwise addition of acetic acid until pH = 5. After that the solvent was evaporated and water (15 mL) was added, and the mixture was extracted with EtOAc (3×10 mL). The combined organic extracts were washed with brine (10 mL), dried over anhydrous Na_2SO_4 and concentrated *in vacuo*. The acquired crude residue was purified by flash column chromatography (EtOAc:hexane: 1:4); to give the title compound (17 mg, 80%) as a yellow solid; m.p. 141 – 143 °C; R_f = 0.32 (EtOAc:hexane: 1:4); ^{1}H NMR (DMSO-d_6, 400 MHz): δ 12.06 (s, 1H), 11.45 (s, 1H), 9.65 (s, 1H), 7.83 (d, J = 9.0 Hz, 1H), 7.46 (dd, J = 8.1, 1.2 Hz, 1H), 7.29 (t, J = 7.9 Hz, 1H), 7.18 (d, J = 8.9 Hz, 1H), 7.08 (dd, J = 7.9, 1.2 Hz, 1H), 3.94 (s, 3H); ^{13}C NMR (DMSO-d_6, 100.6 MHz): δ 157.92, 155.83, 153.30, 132.39, 130.41, 123.95, 123.02, 122.27, 119.41, 108.85, 108.07, 56.27; HRMS (ESI) m/z $[M+H]^+$ calcd. for $C_{12}H_{11}NO_3$ 218.0817, found 218.0824.

9-Methoxynaphtho[1,2-*d*]isoxazole (10): To a solution of 2-hydroxy-8-methoxy-1-naphthaldehyde oxime (10 mg, 0.046 mmol, 1 equiv.) in anhydrous DCM (1 mL), was added AgO (6.3 mg, 0.051 mmol, 1.1 equiv.), *N*-methylmorpholine-*N*-oxide (5.4 mg, 0.046 mmol, 1 equiv.) and a catalytic amount of Et_3N (20 μL). The reaction mixture was left stirring at room temperature for 0.5 h when TLC had shown complete conversion of the starting material.

The reaction mixture was filtered, quenched with water (5 mL) and extracted with DCM (3×5 mL). The combined extracts were washed with brine (5 mL), dried over anhydrous Na_2SO_4 and concentrated *in vacuo*. The acquired crude residue was purified by flash column chromatography (EtOAc:hexane: 1:8) to give the title compound (7 mg, 65%) as a yellow solid; m.p. 99–101 °C; R_f=0.54 (EtOAc: hexane: 1:4); ^{1}H NMR (DMSO-d_6, 400 MHz): δ 9.37 (d, J=1.0 Hz, 1H), 7.97 (d, J=9.0 Hz, 1H), 7.77 (dd, J=9.0, 1.0 Hz, 1H), 7.62 (dd, J=8.2, 1.0 Hz, 1H), 7.52 (t, J=8.0 Hz, 1H), 7.12 (dd, J=7.8, 1.0 Hz, 1H), 4.16 (s, 3H); ^{13}C NMR (DMSO-d_6, 100.6 MHz): δ 162.09, 155.30, 148.13, 131.80, 131.32, 125.76, 120.99, 118.55, 114.21, 110.76, 107.08, 55.69; HRMS (ESI) m/z $[M+H]^+$ calcd. for $C_{12}H_{10}NO_2$ 200.0712, found 200.0712.

(±)-Spiro{naphthalene-1(2*H*),4′-(naphtho[2′,1′:2,3]pyrano[4,5-*c*]furazan)}-2-one-11′-oxide (5): To a solution of (*E*)-2-hydroxy-1-naphthaldehyde oxime (0.2 g, 1.1 mmol), in anhydrous DCM (5 mL), was added AgO (1.30 g, 5.6 mmol), *N*-methylmorpholine-*N*-oxide (0.125 g, 1.1 mmol) and a catalytic amount of Et_3N (20 μL). The reaction mixture was left stirring at room temperature for 1 h after which TLC had shown complete conversion of the starting material. The reaction mixture was then filtered, quenched with water (20 mL) and extracted with DCM (3×15 mL). The combined extracts were washed with brine (15 mL), dried over anhydrous Na_2SO_4 and concentrated *in vacuo*. The acquired crude residue was purified by flash column chromatography (EtOAc:hexane: 1:8) to give the title compound (0.16 g, 40%) as a yellow solid; m.p. 212–214 °C (lit. [7] 211–214 °C); R_f=0.39 (EtOAc:hexane: 1:4); identical in all respects to an authentic sample prepared by Varvounis and co-workers;[7] ^{1}H NMR (DMSO-d_6, 400 MHz): δ 8.83 (d, J=8.5 Hz, 1H), 8.19 (d, J=9.0 Hz, 1H), 8.06 (d, J=8.2 Hz, 1H), 7.96 (d, J= 0.0 Hz, 1H), 7.85–7.75 (m, 2H), 7.71 (d, J=7.6 Hz, 1H), 7.66–7.58 (m, 2H), 7.54 (t, J=7.6 Hz, 1H), 7.34 (d, J=9.0 Hz, 1H); 13 C NMR (DMSO-*d*6, 100.6 MHz): δ 190.69, 154.45, 149.29, 148.28, 135.45, 132.91, 131.42, 131.33, 130.57, 130.47, 129.90, 129.53, 129.43, 129.14, 128.61, 125.68, 124.66, 122.39, 118.17, 108.67, 103.34, 76.51.

Computational Details

All structures involved in the *inter*molecular self-cyclization of *o*-naphthoquinone nitrosomethide **3** with the Ag_2O, AgO and $Pb(OAc)_4$ oxidants were fully geometry-optimized by DFT calculations in the gas phase and in THF and CH_2Cl_2 solvents. The B3LYP functional[67,68] was employed in conjunction with the 6-311G+(d,p)[69] basis set for the C, N, O and H atoms, i.e., a valence triple zeta+polarization on all atoms+diffuse on nonhydrogen atoms, and the Hay-Wadt LANL2DZ ECP[70] basis set for the Pb atoms, i.e., a pseudopotential for the core electrons (up to 5d electrons) and a double-quality basis set for the four outer electrons ($6s^26p^2$). The effectiveness of the adopted method has been checked and proved adequate for the intramolecular cyclization of *o*-naphthoquinone β-nitrosomethides.[9] Frequencies were calculated for all structures to check if they are true minima or not and thermochemical data were also obtained. Moreover, to check the reliability of DFT calculations, single points 2nd order Møller–Plesset perturbation theory (MP2), truncated 4th order perturbation theory (MP4SDQ) and coupled cluster+single+double (CCSD) calculations were carried out in the DFT optimized geometries. Finally, MP2 geometry optimization were carried, showing almost the same geometries and energetics with DFT (B3LYP) methodology.

For the calculations in THF and CH_2Cl_2 solvents, the polarizable continuum model was employed.[71] This model is divided into a solute part, the dye, lying inside a cavity, surrounded by the solvent part. This method reproduces solvent effects quite well.[71]

All calculations were performed using the Gaussian 16 program package.[72] Absolute energies and geometries of the calculated structures are given in SI.

Conflict of Interest

The authors declare no conflict of interest.

Data Availability Statement

The data that support the findings of this study are available in the supplementary material of this article.

Keywords: cycloaddition · DFT calculations · oxidation · oximes · spiro naphthoquinone

[1] M. E. Welsch, S. A. Snyder, B. R. Stockwell, *Curr. Opin. Chem. Biol.* **2010**, *14*, 347–361.
[2] a) H. Sun, G. Tawa, A. Wallqvist, *Drug Discovery Today* **2012**, *17*, 310–324; b) G. Hessler, K.-H. Baringhaus, *Drug Discovery Today Technol.* **2010**, *7*, e263-e269.
[3] For instance: a) M. Uyanik, K. Nishioka, R. Kondo, K. Ishihara, *Nat. Chem.* **2020**, *12*, 353–362; b) M. Mayer, M. Pahl, M. Spanka, M. Grellmann, M. Sickert, Ch. Schneider, K. R. Asmis, D. Belder, *Phys. Chem. Chem. Phys.* **2020**, *22*, 4610–4616; c) Y. Xie, B. List, *Angew. Chem. Int. Ed.* **2017**, *56*, 4936–4940; *Angew. Chem.* **2017**, *129*, 5018–5022; d) N. Meisinger, L. Roiser, U. Monkowius, M. Himmelsbach, R. Robiette, *Chem. Eur. J.* **2017**, *23(21)*, 5137–5142; e) Zh. Wang, J. Sun, *Org. Lett.* **2017**, *19*, 2334–2337; f) D. V. Osipov, V. A. Osyanin, Y. N. Klimochkin, *Russ. Chem. Rev.* **2017**, *86*, 625–687; g) E. E. Allen, C. Zhu, J. S. Panek, S. E. Schaus, *Org. Lett.* **2017**, *19*, 1878–1881; h) R.-l. Liu, X.-Zh. Tang, X.-J. Zhang, M. Yan, A. S. C. Chan, *RSC Adv.* **2017**, *7*, 6660–6663; i) A. Jaworski, K. A. Scheidt, *J. Org. Chem.* **2016**, *81*,10145–10153; j) L. Caruana, M. Fochi, L. Bernardi, *Molecules* **2015**, *20*, 11733–11764; k) S. Saha, S. K. Alamsetti, Ch. Schneider, *Chem. Commun.* **2015**, *51*, 1461–1464; l) S. Saha, Ch. Schneider, *Chem. Eur. J.* **2015**, *21*, 2348–2352; m) Zh. Wang, J. Sun, *Synthesis* **2015**, *47*, 3629–3644; n) Zh. Wang, J. Sun, *Synthesis* **2015**, *47*, 3629–3644; o) A. K. Shaikh, A. G. Varvounis, *RSC Adv.* **2015**, *5*, 14892–14896; p) A. K. Shaikh, A. G. Varvounis, *Org. Lett.* **2014**, *16*, 1478–1481.
[4] a) V. A. Osyanin, A. V. Lukashenko, D. V. Osipov, *Russ. Chem. Rev.* **2021**, *90*, 324–373; b) A. T. Balaban, *Chem. Rev.* **2004**, *104*, 2777–2812; c) P. von Ragué Schleyer, F. Pühlhofer, *Org. Lett.* **2002**, *4*, 2873–2890; d) A. R. Katritzky, K. Jug, D. C. Oniciu, *Chem. Rev.* **2001**, *101*, 1421–1450.
[5] a) D. Liao, H. Li, X. Lei, *Org. Lett.* **2012**, *14*, 18–21 and references cited therein; b) R. M. Jones, C. Selenski, T. R. R. Pettus, *J. Org. Chem.* **2002**, *67*, 6911–6915 (see ref 5, A. B. Turner, *Q. Rev. Chem. Soc.* **1964**, *18*, 347–360, cited therein); c) M. Ashram, D. O. Miller, P. E. Georghiou, *J. Chem. Soc. Perkin Trans. 1* **2002**, 1470–1476; d) T. R. Kasturi, S. K. Jayaram, J. A. Sattigeri, P. V. P. Pragnacharyulu, T. N. G. Row, K. Renuka, K. Venkatesan, N. S. Begum, N. Munirattrinam, *Tetrahedron* **1993**, *49*, 7145–7158.
[6] a) A. J. Boulton, P. G. Tsoungas, C. Tsiamis, *J. Chem. Soc. Perkin Trans. 1* **1987**, 695–697; b) A. J. Boulton, P. G. Tsoungas, C. Tsiamis, *J. Chem. Soc. Perkin Trans. 1* **1986**, 1665–1667; c) A. J. Boulton, P. G. Tsoungas, *J. Chem. Soc. Chem. Commun.* **1980**, 421–422.

[7] a) P. Supsana, P. G. Tsoungas, A. Aubry, S. Skoulika, G. Varvounis, *Tetrahedron* **2001**, *57*, 3445–3453; b) P. Supsana, P. G. Tsoungas, G. Varvounis, *Tetrahedron Lett.* **2000**, *41*, 1845–1847.
[8] P. Kozielewicz, P. G. Tsoungas, D. Tzeli, I. D. Petsalakis, M. Zloh, *Struct. Chem.* **2014**, *25*, 1711–1723.
[9] D. Tzeli, P. G. Tsoungas, I. D. Petsalakis, P. Kozielewicz, M. Zloh, *Tetrahedron* **2015**, *71*, 359–369.
[10] a) A. Marwaha, P. Singh, M. P. Mahajan, *Tetrahedron* **2006**, *62*, 5474–5486; b) P. G. Tsoungas, *Heterocycles* **2002**, *57*, 915–953 and references cited therein; c) P. G. Tsoungas, *Heterocycles* **2002**, *57*, 1149–1178 and references cited therein; d) I. N. Davies, V. A. Gurner, K. N. Houk, *Org. Lett.* **2004**, *6*, 743–746 and references cited therein.
[11] a) P. Pande, J. Shearer, J. Yang, W. A. Greenberg, S. E. Rokita, *J. Am. Chem. Soc.* **1999**, *121*, 6775–6776; b) S. E. Rokita, J. Yang, P. Pande, W. A. Greenberg, *J. Org. Chem.* **1997**, *62*, 3010–3012.
[12] a) Y. Lam, T. B. Ng, R. M. Yao, J. Shi, K. Xu, S. Cho, W. Sze, K. Y. Zhang, *Evid.-Based Complement. Altern. Med.* **2015**, Article ID341752; b) N. Müller, *Curr. Opin. Invest. Drugs* **2010**, *11*,31–42.
[13] G. Pairas, F. Perperopoulou, P. G. Tsoungas, G. Varvounis, *ChemMedChem* **2017**, *12*, 408–419.
[14] a) M. Husband, V. Mehta, *Contin. Educ. Anaesth. Crit. Care Pain* **2013**, *13*, 131–135; b) S. Arfaie, A. Zarghi, *Eur. J. Med. Chem.* **2010**, *45*, 4013–4017; c) K. N. Rainsford, Antiinflammatory Drugs of the 21st Century, chapter 1, in "Inflammation in the Pathogenesis of Chronic Diseases", Ed. R. E. Harris, Springer, **2007**.
[15] V. V. Mezheritskii, V. V. Tkachenko, *Peri Annelated Heterocycles*, p. 67, Academic Press. **1990**.
[16] a) D. Tzeli, P. Kozielewicz, P. G. Tsoungas, M. Zloh, D. Antonow, I. D. Petsalakis, *ChemistrySelect* **2018**, *3*, 9743–9752; b) D. Tzeli, P. G. Tsoungas, *ChemistrySelect* **2021**, *6*, 951–961.
[17] T. Lee, Y.-D. Gong, *Molecules* **2012**, *17*, 5461–5496.
[18] A. H. F. A. El-Wahab, H. M. Mohamed, A. M. El-Agrody, A. H. Bedair, *Eur. J. Chem.* **2013**, *4*, 467–483.
[19] R. Hosseinzadeh, M. Mohadjerni, M. J. Ardestanian, M. R. Naimi-Jamal, Z. Lasemi, *J. Chem. Sci.* **2014**, *126*, 1081–1089.
[20] B. Lukyanov, G. Vasilyuk, E. Mukhanov, L. Ageev, M. Lukyanova, Y. Alexeenko, S. Besugliy, V. Tkachev, *Int. J. Photoenergy* **2009**, Article ID 689450.
[21] a) K. Hiesinger, D. Darin, E. Proschak, M. Krasavin, *J. Med. Chem.* **2021**, *64*, 150–183; b) E. Chupakhin, O. Babich, Ar. Prosekov, L. Asyakina, M. Krasavin, *Molecules* **2019**, *24*, 4165); c) "Privileged Scaffolds in Medicinal Chemistry, Design, Synthesis, Evaluation," Ed. S. Bräse., RSC Drug Discovery Series No. 50, Chapter 16, *Spirocycles as Privileged Structural Motifs in Medicinal Chemistry*", **2016**.
[22] a) J. Li, L. Li, Y. Si, X. Jiang, L. Guo, Y. Chen, *Org. Lett.* **2011**, *13*, 2670–2672; b) C. Tu, E. A. Osborne, A. Y. Louie, *Tetrahedron* **2009**, *65*, 1241–1246; c) H. Fujimoto, M. Nozawa, E. Okuyama, M. Ishibashi, *Chem. Pharm. Bull.* **2002**, *50*, 330–336.
[23] a) Sh. Chen, Q. Bian, P. Wang, X. Zheng, L. Lv, Zh. Dang, G. Wang, *Polym. Chem.* **2017**, *8*, 6150–6157; b) L. Zhang, Zh. Yang, W. Zhu, Zh. Ye, Y. Yu, Z. Xu, J. Ren, P. Li, *ACS Biomater. Sci. Eng.* **2017**, *3*, 1690–1701.
[24] R. Klajn, *Chem. Soc. Rev.* **2014**, *43*, 1–488 and references cited therein.
[25] a) W. Yuan, X. Gao, E. Pei, Zh. Li, *Polym. Chem.* **2018**, *9*, 3651–3661; b) S. van de Linde, M. Sauer, *Chem. Soc. Rev.* **2014**, *43*, 1076–1089 and references cited therein.
[26] a) O. Talhi, D. C. G. A. Pinto, F. A. Almeida Paz, M. Hamdi, A. M. S. Silva, *Synlett* **2015**, *26*, 167–172; b) R. Hosseinzadeh, M. Mohadjerani, M. J. Ardestanian, M. R. Naimi-Jamal, Z. Lasemi, *J. Chem. Sci.* **2014**, *126*, 1081–1089; c) A. H. F. Abd El Wahab, H. M. Mohamed, A. M. El Agrody, A. H. Bedair, *Eur. J. Chem.* **2013**, *4*, 467–483; d) Y. Sawama, Y. Shishido, T. Yanase, K. Kawamoto, R. Goto, Y. Monguchi, Y. Kita, H. Sajiki, *Angew. Chem. Int. Ed.* **2013**, *52*, 1515–1519; *Angew. Chem.* **2013**, *125*, 1555–1559.
[27] a) A. Rohadi, S. A. Hasbullah, A. M. Lazim, R. Nordin, *Heterocycles* **2014**, *89*, 1017–1024; b) K. Kruttwig, D. R. Yankelevich, Ch. Brueggemann, Ch. Tu, N. L'Etoile, A. Knoesen, A. Y. Louie, *Molecules* **2012**, *17*, 6605–6624; c) B. Seefeldt, R. Kasper, M. Beining, J. Mattay, J. Arden-Jacob, N. Kemnitzer, K. H. Drexhage, M. Heilemann, M. Sauer, *Photochem. Photobiol. Sci.* **2010**, *9*, 213–220; d) B. Lukyanov, G. Vasilyuk, E. Mukhanov, L. Ageev, M. Lukyanova, Y. Alexeenko, S. Besugliy, V. Tkachev, *Int. J. Photoenergy* **2009**, Article ID 689450.
[28] a) N. Babic, F. Peyrot, *Magnetochemistry* **2019**, *5*, 13; b) S. Suzen, H. Gurer-Orhan, L. Saso, *Molecules* **2017**, *22*, 181.
[29] The spiro adduct **5** is being investigated as a probe for the detection of reactive oxygen and nitrogen species (ROS and RNS) in oxidative stress conditions and a source for a) symmetrically 3,4-diaryl substituted furoxans (through reductive or nucleophilic pyran cleavage of **5**).
[30] J.-P. Finet, Tetrahedron Organic Chemistry Series: Ligand Coupling Reactions with Heteroatomic Compounds, Vol. 18, Pergamon: Oxford, **1998**.
[31] P. G. Tsoungas, A. Diplas, *Heteroat. Chem.* **2003**, *14(7)*, 642–670.
[32] a) A. Yoshimura, V. V. Zhdankin, *Arkivoc* **2017**, *(i)*, 99–116; b) A. Yoshimura, V. V. Zhdankin, *Chem. Rev.* **2016**, *116(5)*, 3328–3435; c) A. Yoshimura, K. C. Nguyen, S. C. Klasen, P. S. Postnikov, M. S. Yusubov, A. Saito, V. N. Nemykin, V. V. Zhdankin, *Asian J. Org. Chem.* **2016**, *5(9)*, 1128–1133; d) F. Berthiol, *Synthesis* **2015**, *47(5)*, 587–603; e) V. V. Zhdankin, *Hypervalent Iodine Chemistry: Preparation, Structure and Synthesis Applications of Polyvalent Iodine Compounds*, Wiley, **2013**; f) F. V. Singh, T. Wirth, *Synthesis* **2013**, *45*, 2499–2511.
[33] a) Y. Shimoyama, T. Kojima, *Inorg. Chem.* **2019**, *58*, 9517–9542; b) G. Frenking, S. Shaik, in "The Chemical Bond: Chemical Bonding Across the Periodic Table", Wiley-VCH, Verlag GmbH & Co, KGaA Boschstr., 12 69469, Weinheim, Germany, **2014**; c) W. Levason, M. D. Spicer, *Coord. Chem. Rev.* **1987**, *76*, 45–120.
[34] C. Dolka, K. Van Hecke, L. Van Meervelt, P. G. Tsoungas, G. Varvounis, *Org. Lett.* **2009**, *11*, 2964–2967.
[35] A. Edgars, A. Ramona, *Curr. Org. Synth.* **2014**, *11(3)*, 403–428.
[36] N. Z. Burns, P. S. Baran, R. W. Hoffmann, *Angew. Chem. Int. Ed.* **2009**, *48*, 2854–2867; *Angew. Chem.* **2009**, *121*, 2896–2910.
[37] Dearomatization, under (non)oxidative conditions, currently a vibrant research area, represents an efficient route for the construction of spirocyclic enones of controlled regio-, (dia)stereo- and enantioselectivity, frequently found in bioactive natural products and therapeutics. For indicative most recent reports see: a) M. Dekhici, S. Plihon, N. Bar, D. Villemin, H. Elsiblani, N. Cheikh, *ChemistrySelect* **2019**, *4*, 705–708; b) M. Jin, W. Ren, D.-W. Qian, Sh.-D. Yang, *Org. Lett.* **2018**, *20*, 7015–7019; c) H.-F. Tu, C. Zheng, R.-Q. Xu, X.-J. Liu and S.-L. You, *Angew. Chem. Int. Ed.* **2017**, *56*, 3237–3241; *Angew. Chem.* **2017**, *129*, 3285–3289; d) D. Shen, Q. Chen, P. Yan, X. Zeng and G. Zhong, *Angew. Chem. Int. Ed.* **2017**, *56*, 3242–3246; *Angew. Chem.* **2017**, *129*, 3290–3294; e) N. Jain, S. Xu, M. A. Ciufolini, *Chem. Eur. J.* **2017**, *23*, 4542–4546; f) "Asymmetric Oxidative Dearomatization Reaction": M. Uyanik, K. Ishihara in *Asymmetric Dearomatization Reactions*, Ed., S.-L. You, Chapter 6, pp. 129–152, Wiley VCH, Weinheim, **2016**.
[38] a) B. Maes, J. Cossy, S. Polanc, O. V. Larionov in "Topics in Heterocyclic Chemistry 53: Heterocyclic N-Oxides", Series editors, Springer International Publishing, **2017**; b) Y. Wang, L. Zhang, *Synthesis* **2015**, *47*, 289–305; c) T. Pasinszki, N. P. C. Westwood, *Curr. Org. Chem.* **2011**, *15*, 1720–1733; d) Z. X. Yu, P. Caramella, K. N. Houk, *J. Am. Chem. Soc.* **2003**, *125*,15420–15425. G. Rauhut, *J. Org. Chem.* **2001**, *66*, 5444–5448.
[39] Y. Tanoue, K. Sakata, M. Hashimoto, Sh.-I. Morishita, M. Hamada, N. Kai, T. Nagai, *Tetrahedron* **2002**, *58*, 99–104.
[40] a) A. Patel, T. Netcher, T. Rosenau, *Tetrahedron Lett.* **2008**, *49*, 2442–245; b) T. Rosenau, K. Mereiter, C. Jäger, P. Schmidt, P. Cosma, *Tetrahedron* **2004**, *60*, 5719–5723; c) T. Rosenau, A. Potthast, T. Elder, P. Cosma, *Org. Lett.* **2002**, *4*, 4285–4288.
[41] Some *o*-quinone methides have been "stabilized" to a sufficiently long lifetime to allow their study directly. For examples see: a) T. K. Venkatachalam, G. K. Pierens, M. R. Campitelli, D. C. Reutens, *Magn. Reson. Chem.* **2010**, *48*, 585–592); b) N. Basarić, I. Žabčić, K. Mlinarič, P. Wan, *J. Org. Chem.* **2010**, *75*, 102–116; c) H. Amouri, J. LeBras, *Acc. Chem. Res.* **2002**, *35*, 501–510; d) A. Vigalok, D. Milstein, *Acc. Chem. Res.* **2001**, *34*, 798–807; e) S. M. Stokes Jr, F. Ding, P. L. Smith, J. M. Keane, M. E. Kopach, R. Jervis, M. Sabat, W. D. Harman, *Organometallics* **2003**, *22*, 4170–4171.
[42] T. Pang, Y. Sun, W.-J. Xue, Y.-P. Zhu, G.-A. Yu, A.-X. Wu, *Adv. Synth. Catal.* **2013**, *355*, 2208–2216.
[43] D. Liao, H. Li, X. Lei, *Org. Lett.* **2012**, *14*, 18–21.
[44] PCET (HAT or CPET), taking place intra- or intermolecularly, are very important processes in Chemistry and Biology with diverse applications, see a) J. M. Guevara-Vela, M. Gallegos, M. A. Valentín-Rodríguez, A. Costales, T. Rocha-Rinza, Á. M. Pendás, *Molecules* **2021**, *26*, 4196; b) Zh. Zijie, K. Xiangmei, L. Tianfei, *Chin. J. Org. Chem.* **2021**, *41*, 3844–3879; c) W. D. Morris, J. M. Mayer, *J. Am. Chem. Soc.* **2017**, *139*, 10312–10319; d) Sh. Hammes-Schiffer, *J. Am. Chem. Soc.* **2015**, *137*, 8860–8871; e) J. Bonin, C. Costentin, M. Robert, J.-M. Saveant, C. Tard, *Acc. Chem. Res.* **2012**, *45*, 372–381; f) J. M. Mayer, *Acc. Chem. Res.* **2011**, *44*, 36–46.
[45] a) S. J. Mora, E. Odella, G. F. Moore, D. Gust, T. A. Moore, A. L. Moore, *Acc. Chem. Res.* **2018**, *51*, 445–453; b) J. W. Darcy, B. Koronkiewicz, G. A. Parada, J. M. Mayer, *Acc. Chem. Res.* **2018**, *51*, 2391–2399; c) D. R.

Weinberg, C. J. Gagliardi, J. F. Hull, C. F. Murphy, C. A. Kent, B. C. Westlake, A. Paul, D. H. Ess, D. G. McCafferty, T. J. Meyer, *Chem. Rev.* **2012**, *112*, 4016–4093; d) C. Costentin, M. Robert, J.-M. Savéant, *Chem. Rev.* **2010**, *110*, PR1–PR40.

[46] a) J. E. M. N. Klein, G. Knizia, *Angew. Chem. Int. Ed.* **2018**, *57*, 11913–11917; *Angew. Chem.* **2018**, *130*, 12089–12093; b) Q. Wang, Y. Niu, R. Wang, H. Wu, Y. Zhang, *Chem. Asian J.* **2018**, *13*, 1735–1743; c) T. F. Markle, A. L. Tenderholt, J. M. Mayer, *J. Phys. Chem. B.* **2012**, *116*, 571–584; d) A. Sirjoosingh, Sh. Hammes-Schiffer, *J. Phys. Chem. A* **2011**, *115*, 2367–2377; e) J. M. Mayer, *Acc. Chem. Res.* **2011**, *44*, 36–46.

[47] a) M. Dolai, U. Saha, *Heliyon* **2020**, *6*, e04942; b) Z. Feng, Sh. Jia, H. Chen, L. You, *Tetrahedron* **2020**, *76*, 131128; c) T. Kojima, *Bull. Chem. Soc. Jpn.* **2020**, *93*, 1571–1582; d) A. Tarai, J. B. Baruah, *ChemistrySelect* **2018**, *3*, 11406–11413; e) A. Tarai, J. B. Baruah, *CrystEngComm* **2015**, *17*, 2301–2309; f) C. B. Aakeröy, A. S. Sinha, K. N. Epa, P. D. Chopade, M. M. Smith, J. Desper, *Crystal Growth & Design* **2013**, *13*, 2687–2695; g) I. S. K. Kerkines, I. D. Petsalakis, G. Theodorakopoulos, J. Rebek, Jr., *J. Phys. Chem. A* **2011**, *115*, 834–840.

[48] L. Cai, Q. Sun, M. Bao, H. Ma, Ch. Yuan, W. Xu, *ACS Nano* **2017**, *11*, 3727–3732.

[49] a) W. Zierkiewicz, M. Michalczyk, S. Scheiner, *Molecules* **2021**, *26*, 1740; b) J. H. Stenlid, A. J. Johansson, T. Brinck, *Phys. Chem. Chem. Phys.* **2018**, *20*, 2676–2692; c) J. H. Stenlid, T. Brinck, *J. Am. Chem. Soc.* **2017**, *139*, 11012–11015.

[50] π-Delocalization in the chelate ring may raise IMHB energy by as much as 30% and more so in the Transition State J.-D. Yang, P. Ji, X.-S. Xue, J.-P. Cheng, *J. Am. Chem. Soc.* **2018**, *140*, 8611–8623.

[51] For RAHB (and its criticism) see: a) M. Domagała, S. Simon, M. Palusiak, *Int. J. Mol. Sci.* **2022**, *23*, 233 and specific references cited therein; b) S. J. Grabowski, *Crystals* **2021**, *11*, 5; c) A. Jezierska, P. M. Tolstoy, J. J. Panek, A. Filarowski, *Catalysts* **2019**, *9*, 909; d) X. Jiang, H. Zhang, W. Wu, Y. Mo, *Chem. Eur. J.* **2017**, *23*, 1–8; e) G. Gilli, P. Gilli, The Nature of the Hydrogen Bond. In Outline of a Comprehensive Hydrogen Bond Theory; Oxford University Press: Oxford, UK, **2009**; f) J.-D. Yang, P. Ji, X.-S. Xue, J.-P. Cheng, *J. Am. Chem. Soc.* **2018**, *140*, 8611–8623.

[52] a) R. S. da Silva, M. Y. Ballester, *Chem. Phys.* **2022**, *557*, 111480; b) AgO is a mixed Ag(I) (d^{10}) and Ag(III) (d^8) oxide, see ref 30 herein and E. V. Trushin, I. L. Zilberberg, *Chem. Phys. Lett.* **2013**, *560*, 37–41; c) L. P. Wolters, F. M. Bickelhaupt, *ChemistryOpen* **2013**, *2*, 106–114; d) Encyclopedia of Inorganic Chemistry, John Wiley Ltd., **2006**.

[53] a) O. I. Siidra, S. V. Krivovichev, S. K. Filatov, *Z. Kristallogr.* **2008**, *223*, 114–125; b) F. Pei, S. Wu, G. Wang, M. Xu, S.-Y. Wang, L.-Y. Chen, *J. Korean Phys. Soc.* **2009**, *55*, 1243–1249; c) I. Persson, K. B. Nilsson, *Inorg. Chem.* **2006**, *45*, 7428–7434; d) K. Aoki, K. Murayama, N.-H. Hu, *Met. Ions Life Sci.* **2017**, *17*, 123–199.

[54] F. Li, Y. Zhou, H. Yang, Z. Wang, Q. Yu, F.-L. Zhang, *Org. Lett.* **2019**, *21*, 3692–3695.

[55] a) M. Hggle, X. Lucas, D. Ostrovskyi, P. Regenass, S. Gerhardt, O. Einsle, M. Hau, M. Jung, B. Breit, S. Ggnther, D. Wohlwend, *Angew. Chem. Int. Ed.* **2017**, *56*, 12476–12480 (see SI, structure **18**, S16 therein); b) V. V. Mezheritskii, *Russ. Chem. Rev.* **2011**, *80(1)*, 1–49.

[56] a) A. S. Negi, S. K. Chattopadhyay, *Synth. Commun.* **2005**, *35*, 15–21; b) M. Pittelkow, U. Boas, M. Jessing, K. J. Jensen, J. B. Christensen, *Org. Biomol. Chem.* **2005**, *3*, 508–514; c) U. Boas, J. B. Christensen, K. J. Jensen, *J. Comb. Chem.* **2004**, *6*, 497–503; d) U. Boas, J. Brask, J. B. Christensen, K. J. Jensen, *J. Comb. Chem.* **2002**, *4*, 223–228; e) J. P. Deville, V. Behar, *J. Org. Chem.* **2001**, *66*, 4097–4098.

[57] T. J. Dale, A. C. Sather, J. Rebek, Jr, *Tetrahedron Lett.* **2009**, *50*, 6173–6175.

[58] a) L. R. Gomes, M. V. N. de Souza, C. F. Da Costa, J. L. Wardell, J. Nicolson Low, *Acta Crystallogr.* **2018**, *E74*, 1480–1485; b) L. Sobczyk, D. Chudoba, P. M. Tolstoy, A. Filarowski, *Molecules* **2016**, *21*, 1657.

[59] a) J. Sączewski, M. Gdaniec, *Eur. J. Org. Chem.* **2010**, 2387–2394; b) T. J. Dale, A. C. Sather, J. Rebek Jr, *Tetrahedron Lett.* **2009**, *50*, 6173–6175; c) A. Pace, I. Pibiri, A. Palumbo Piccionello, S. Buscemi, N. Vivona, G. Barone, *J. Org. Chem.* **2007**, *72*, 7656–7666; d) A. Bottoni, V. Frenna, C. Z. Lanza, G. Macaluso, D. Spinelli, *J. Phys. Chem. A* **2004**, *108*, 1731–1740; e) M. Searcey, S. S. Grewal, F. Madeo, P. G. Tsoungas, *Tetrahedron Lett.* **2003**, *44*, 6745–6747.

[60] a) M. Dolai, T. Mistri, S. Biswas, G. Rogez, M. Ali, *ChemPlusChem* **2014**, *79*, 1649–1656; b) K. N. Lazarou, A. K. Boudalis, V. Psycharis, C. P. Raptopoulou, *Inorg. Chim. Acta* **2011**, *370*, 50–58.

[61] a) Zh. Chen, C. Han, C. Fan, G. Liu, Sh. Pu, *ACS Omega* **2018**, *3*, 8160–8168; b) E. Sanchez, S. Lu, C. Reed, J. Schmidt, M. Forconi, *J. Phys. Org. Chem.* **2016** *29*, 185–189; c) E. Whiting, M. E. Lanning, J. A. Scheenstra, S. Fletcher, *J. Org. Chem.* **2015**, *80*, 1229–1234. S. Fletcher, *Org. Chem. Front.* **2015**, *2*, 739–752.

[62] a) A. D. Becke, *J. Chem. Phys.* **1993**, *98*, 1372–1377; b) C. Lee, W. Yang, R. G. Parr, *Phys. Rev. B.* **1988**, *37*, 785–789.

[63] a) Y. Bh. Pandit, R. L. Sahani, R.-Sh. Liu, *Org. Lett.* **2018**, *20*, 6655–6658; b) T. Noguchi, Y. Nishii, M. Miura, *Chem. Lett.* **2017**, *46*, 1512–1514; c) Y.-P. Han, X.-S. Li, Z. Sun, X.-Y. Zhu, M. Li, X.-R. Song, Y.-M. Liang, *Adv. Synth. Catal.* **2017**, *359*, 2735–2740.

[64] P. Franchi, M. Lucarini, G. Franco Pedulli, L. Valgimigli, B. Lunelli, *J. Am. Chem. Soc.* **1999**, *121*, 507–514.

[65] Strong intramolecular H bonds are disrupted by Na but not K or Rb ions, see J. A. Berenbeim, N. G. K. Wong, M. C. R. Cockett, G. Berden, J. Oomens, A. M. Rijs, C. E. H. Dessent, *Phys. Chem. Chem. Phys.* **2020**, *22*, 19522–19531; Y. Song, D. Shen, Q. Zhang, B. Chen, G. Xu, *Tetrahedron Lett.* **2014**, *55*, 639–641.

[66] K. Acosta-Quiroga, C. Rojas-Peña, L. S. Nerio, M. Gutiérrez, E. Polo-Cuadrado, *RSC Adv.* **2021**, *11*, 21926–21954.

[67] A. Morgenstern, T. R. Wilson, M. E. Eberhart, *J. Phys. Chem. A* **2017**, *121*, 4341–4351.

[68] L. A. Curtiss, M. P. McGrath, J.-P. Blandeau, N. E. Davis, R. C. Binning, Jr., L. Radom, *J. Chem. Phys.* **1995**, *103*, 6104–6113.

[69] P. J. Hay, W. R. Wadt, *J. Chem. Phys.* **1985**, *82*, 299–310.

[70] M. Cozi, G. Scalmani, N. Rega, V. Barone, *J. Chem. Phys.* **2002**, *117*, 43–54.

[71] J. Tomasi, B. Mennucci, R. Cammi, *Chem. Rev.* **2005**, *105*, 2999–3094; A. Pedone, J. Bloino, S. Monti, G. Prampolini, V. Barone, *Phys. Chem. Chem. Phys.* **2010**, *12*, 1000–1006.

[72] Gaussian16, Revision C.01, M. J. Frisch, G. W. Trucks, H. B. Schlegel, G. E. Scuseria, M. A. Robb, J. R. Cheeseman, G. Scalmani, V. Barone, G. A. Petersson, H. Nakatsuji, X. Li, M. Caricato, A. V. Marenich, J. Bloino, B. G. Janesko, R. Gomperts, B. Mennucci, H. P. Hratchian, J. V. Ortiz, A. F. Izmaylov, J. L. Sonnenberg, D. Williams-Young, F. Ding, F. Lipparini, F. Egidi, J. Goings, B. Peng, A. Petrone, T. Henderson, D. Ranasinghe, V. G. Zakrzewski, J. Gao, N. Rega, G. Zheng, W. Liang, M. Hada, M. Ehara, K. Toyota, R. Fukuda, J. Hasegawa, M. Ishida, T. Nakajima, Y. Honda, O. Kitao, H. Nakai, T. Vreven, K. Throssell, J. A. Montgomery, Jr., J. E. Peralta, F. Ogliaro, M. J. Bearpark, J. J. Heyd, E. N. Brothers, K. N. Kudin, V. N. Staroverov, T. A. Keith, R. Kobayashi, J. Normand, K. Raghavachari, A. P. Rendell, J. C. Burant, S. S. Iyengar, J. Tomasi, M. Cossi, J. M. Millam, M. Klene, C. Adamo, R. Cammi, J. W. Ochterski, R. L. Martin, K. Morokuma, O. Farkas, J. B. Foresman, and D. J. Fox, Gaussian, Inc., Wallingford CT, **2016**.

Manuscript received: September 12, 2022
Revised manuscript received: November 22, 2022
Accepted manuscript online: November 23, 2022